New Journal of Physics
The open-access journal for physics

Influence of fabrication errors on wake function suppression in NC X-band accelerating structures for linear colliders

R M Jones[1,2], C E Adolphsen[3], R H Miller[3], J W Wang[3] and T Higo[4]

[1] The University of Manchester, Manchester M13 9PL, UK
[2] Cockcroft Institute, Daresbury, WA4 4AD, UK
[3] SLAC National Accelerator Laboratory, CA 94309, USA
[4] KEK, National Laboratory for High Energy Physics, Tsukuba-shi, Japan
E-mail: roger.jones@manchester.ac.uk

New Journal of Physics **11** (2009) 033013 (13pp)
Received 8 January 2009
Published 10 March 2009
Online at http://www.njp.org/
doi:10.1088/1367-2630/11/3/033013

Abstract. Wake function suppression is effected by ensuring that the mode frequencies of an X-band normal conducting (NC) accelerating structure of multiple cells are detuned and moderately damped by waveguide manifolds attached to the outer wall of the accelerator. We report on the dilution in the wake function suppression that occurs due to errors resulting from the fabrication process. After diffusion bonding 206 cells a non-uniform expansion in the cell geometry forces a substantial shift in the frequencies of select cells. We remap all circuit parameters to these shifted cell frequencies to predict the wake function. Experiments performed on the SLC at the SLAC National Accelerator Laboratory indicate that the wake function is well predicted by the circuit model.

Contents

1. Introduction 2
2. Fabrication errors and their influence on mode frequencies 4
3. Analysis of the spectral function and the wake function 5
4. Fabrication errors and their influence on wake functions 9
Acknowledgments 12
References 13

1. Introduction

Linear accelerators for collider [1]–[5] and light source [6] applications necessitate the fabrication of accelerating cavities, each of which consists of several cells, to provide acceleration of the main particle beams. For the next generation of linear colliders there are two main options under consideration, one of which consists of superconducting (SC) cavities [7] and the other consists of normal conducting (NC) cavities [4, 5]. The SC option aims at an operational accelerating gradient of 31.5 MV m^{-1} at an L-band frequency of 1.3 GHz and the NC design for CLIC [4, 5] will have a gradient of 100 MV m^{-1} at an X-band frequency of 12 GHz. The higher frequency of the NC design results in a relatively compact accelerator, which incorporates considerably smaller irises than that of the SC design. However, in order to maintain a high beam quality with commensurate beam stability, the electromagnetic field must be precisely maintained. The geometry of the cavity and radio frequency (RF) source determine the electromagnetic field. Consequently, fabrication and alignment tolerance issues are considerably more severe in NC linacs.

In addition to the main accelerating mode, the passage of a relativistic particle beam through the accelerating cavities readily results in the excitation of parasitic modes, which if left unchecked can dilute a quantity known as the emittance of the beam [8]. This parameter describes the beam quality and within a given accelerator it must be preserved for linear collider or light source applications. The collection of modes excited by the beam corresponds to the electromagnetic field experienced by the beam. For a particle beam travelling close to the speed of light this electromagnetic field is conveniently represented as a wake function [9], which has both longitudinal and transverse components. The former affects the energy spread in the beam and the latter, the transverse emittance and can result in a beam break up (BBU) instability [10]–[12].

In this paper, we study the transverse wake function suppression in an X-band accelerating cavity where the influence of wake functions is markedly more severe than its L-band counterpart. In particular, we present results on an accelerating structure known as Rounded Damped Detuned Structure version 1 (RDDS1), which was designed and fabricated at SLAC and KEK. The structure was optimized with respect to maximizing the shunt impedance of the accelerating mode. It was also provided with the wake function suppression obtained by detuning each of the cells of the accelerating cavity and, by moderate wake function damping, effected by four attached manifolds. A cross-section of this accelerating structure is illustrated schematically in figure 1. The main features including accelerating cells and attached power couplers and dampers are evident.

In reality, it consists of 206 cells in which the iris of each cell is carefully tapered with an erf (error function) distribution. This tapering in the cell geometry provides a wake function that decays with the envelope approximated by a Gaussian function [13]. Detuning the cell frequencies succeeds in damping the wake function over a limited number of bunches until eventually the wake function recoheres and rises at this point. The attached manifolds damp down the wake function to prevent the recoherence and the corresponding Q is $\sim$500. The manifolds allow the electromagnetic field to be coupled via slots through each accelerating cell apart from the first and last three cells, which are missing coupling slots due to mechanical design considerations. The final X-band RDDS1, fabricated by diffusion bonding of 206 cells that have been machined with a computer-controlled ultra high-precision lathe equipped with a diamond point tool cutting head, are illustrated in figure 2. There are three collars, one in the

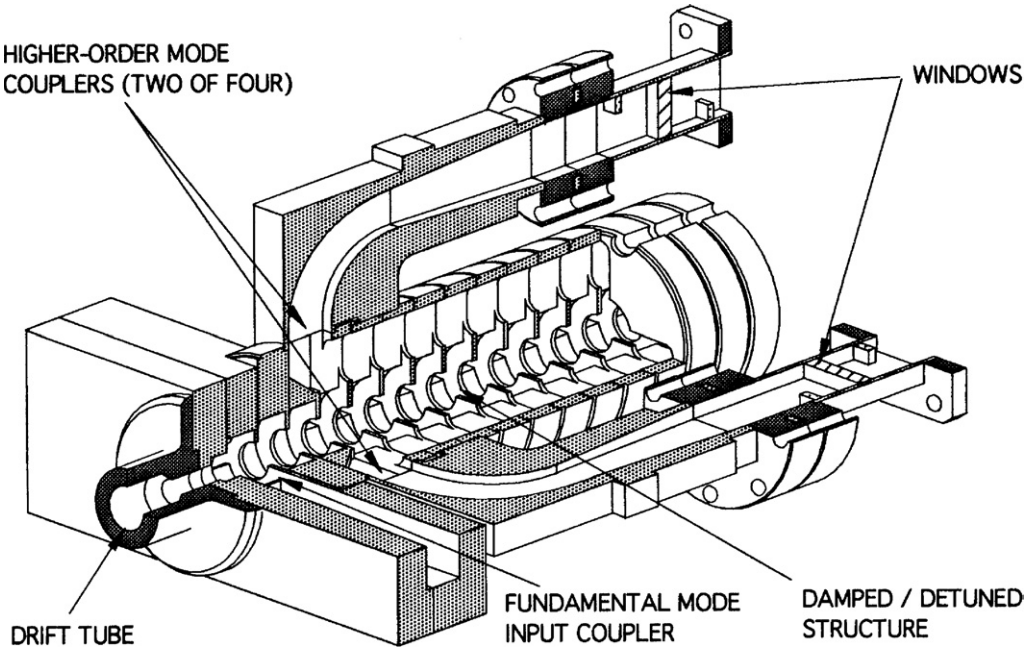

Figure 1. Schematic CAD representation of a section of RDDS1 accelerating linac.

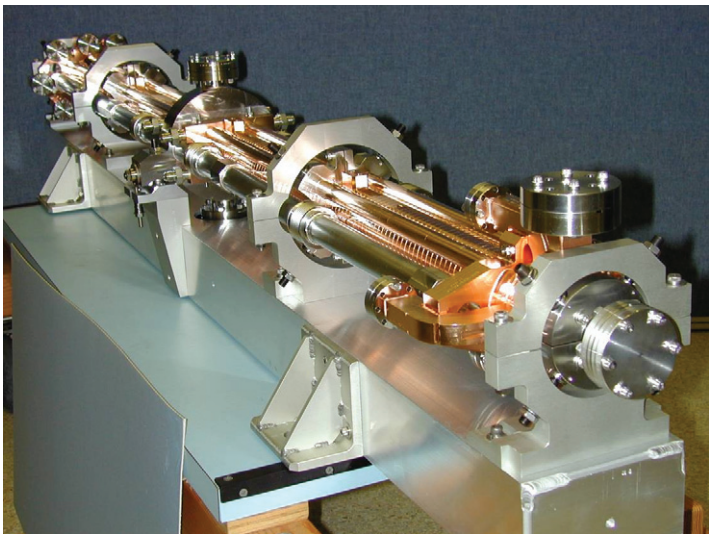

Figure 2. RDDS1 accelerator illustrated with higher order mode (HOM) couplers attached.

middle and one at each end of the accelerator to support the structure and maintain mechanical integrity. However, as these materials are made of stainless steel they had a different expansion coefficient from that of the copper cells. This resulted in the cells in which the supports were located expanding more than those in the bulk of the structure. As the cell frequencies are strongly related to cell geometry, an expansion of the cells is liable to modify these frequencies. Furthermore, the mode frequencies (which result from joining the cells together in a complete structure) are also modified by geometrical errors. We performed simulations to predict the

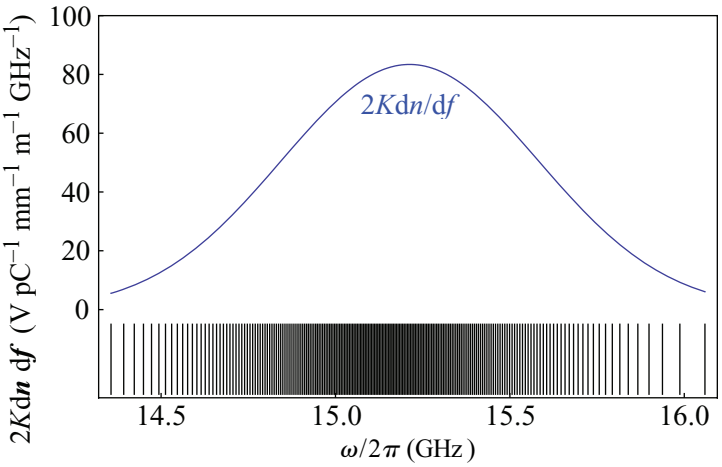

Figure 3. Twice the smoothed undamped kick factor weighted density function, $2K\,\mathrm{d}n/\mathrm{d}f$ (in blue) together with the location of individual modes (indicated by vertical black lines).

wake function due to these frequency errors, and we made an experimental measurement in the ASSET facility (see figure 8) of the SLAC National Accelerator Laboratory linac.

This paper is organized such that the frequency shift introduced by fabrication errors is discussed in the next section, followed by a section analysing the wake function with a spectral function technique and the final section discusses the theoretical prediction of the wake function and compares it with experimentally determined values from the SLAC linac. The final section also presents some conclusions and recommendations for the design of future structures for CLIC and similar collider applications.

2. Fabrication errors and their influence on mode frequencies

This work deals with the implications of shift in the cell frequencies for the damping of the transverse wake function experienced by the beam. Individual cell frequencies, together with $K\,\mathrm{d}n/\mathrm{d}f$, the product of the cell kick factor (a measure transverse momentum imparted to trailing bunches [9]) with the mode density function are illustrated in figure 3 for the structure. As $K\,\mathrm{d}n/\mathrm{d}f$ is designed to be a Gaussian profile, then the wake function will also decay in a Gaussian manner. To understand the impact of fabrication errors on wake function we note that the separation of modes is largest towards the tails of the Gaussian and is in fact larger than 100 MHz in these regions. Furthermore, the modes are more closely spaced towards the centre of the distribution where the minimum spacing is 7 MHz. As the collars introduced geometrical errors for a limited number of cells, a coordinate measurement machine (CMM) was used to ascertain the changes in the outer radius of the cavity and from this the changes to the cell frequencies are inferred. In addition to this, a 'bead-pull' [14] measurement was made on the structure in order to measure the cell frequencies. The frequency shift obtained from the two methods was consistent and the result obtained from the bead-pull measurement is illustrated in figure 4. There are smaller shifts in the frequencies at cells intermediate to the end and mid-cells. However, the end and mid-cell frequency shifts are clearly the largest, as they are 35 and 40 MHz, respectively. These shifts are much larger than the spacing of individual modes in the

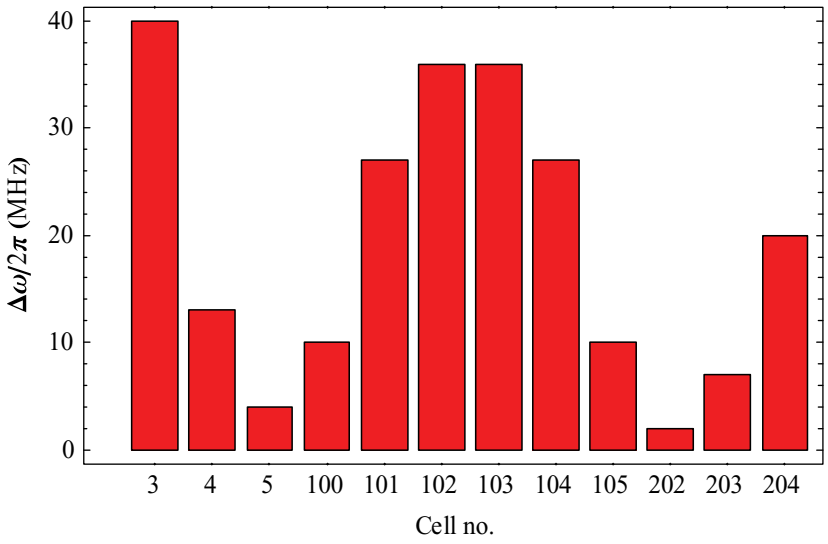

Figure 4. Deviation in cell frequencies from their design values obtained from bead-pull measurements.

centre of the distribution and are likely to have a significant impact on the decay of the wake function, which cannot be considered a perturbation to the original distribution. This flaring of cells in the ends of the structure was largely removed by symmetrical squeezing of the end cells. However, the flaring in the centre was not removed due to time constraints, and hence the effect of this error on the wake function can be studied. To evaluate the wake function, a spectral technique [13] is applied with modified frequencies. This method is discussed in the next section.

3. Analysis of the spectral function and the wake function

In order to assess the transverse momentum imparted to the beam the wake function may be evaluated with large-scale finite element or finite difference computer codes [15]–[17]. However, these codes necessitate large memory and long run times in order to successfully evaluate the fields to sufficient accuracy. These methods do not readily lend themselves to a rapid design of the accelerating structure where many parameters must be varied and the impact of the parameter change must be rapidly assessed. In order to rapidly obtain the wake function a circuit model of the structure is employed [13], based on the model in [18] with the addition of manifolds attached and coupled to the accelerating cells through transverse electric (TE) modes. The circuit model must account for the fact that a series of dipole modes are excited in the multi-cell cavity. These dipole modes are hybrid in character and they consist of a mixture of coupled TE and transverse magnetic (TM) modes. The model, illustrated in figure 5 for three representative cells, takes into account this hybrid character of the modes by coupling the lower TM chain inductively to the upper TE chain. In addition to the TM modes being coupled to their TE neighbours, adjacent cells such as TM modes in cell n are coupled to those in cell $n-1$ and to cell $n+1$. In this model, nearest-neighbour coupling is sufficient to account for the wake function excited in the cavity. The current of the charged particle beam, coupling directly into the capacitance of the nth cell, is indicated by I_n. The upper solid pair of parallel lines denotes

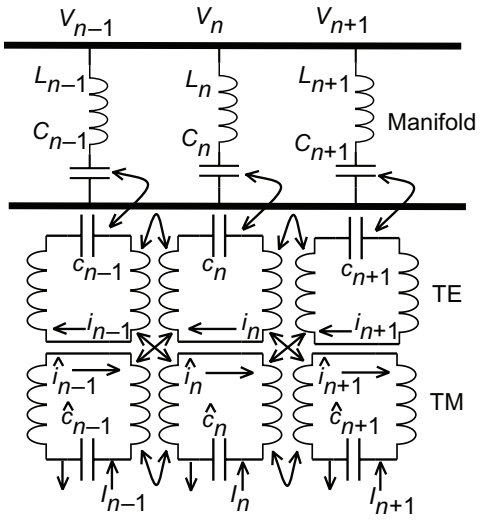

Figure 5. Circuit model of dipole wake function coupled to a waveguide-like manifold.

a transmission line model of the TE waveguide mode in the manifold. This manifold is coupled through a slot in each cell of the accelerator and finite element simulations, conducted on single cells coupled to a manifold through a slot, indicate this coupling is TE in nature. We represent this TE coupling in the circuit model in figure 5 with capacitive coupling. Further details on the manifold coupled to the TE and TM circuit chain are given in [13].

In the application of this circuit model, the parameters of a limited number of cells are obtained from accurate simulations with finite element or finite difference codes and then the remaining cell parameters are obtained by interpolation. In general, eight parameters for each cell are required to characterize the interaction and this is achieved by solving eight coupled non-linear equations from eight points on the characteristic dispersion curves. In summary, the beam couples to the circuit through TM modes and as the modes are dipole in character, TE modes are also excited. The dipole modes are damped by slots cut into the cells and coupled through TE modes to the attached manifolds. The modes of the complete structure may then be obtained from the characteristic eigenvalues and eigenvectors of the system, which the circuit model describes. However, as the coupling is large and the shift due to fabrication errors is also large, an eigenvalue approach is not sufficient. For this reason, we use a spectral function method [13] that essentially consists of forming the impedance of the cavity and then taking the Fourier transform of this impedance in order to obtain the wake function. This method is able to accommodate large frequency shifts, Ohmic losses and strong mode coupling.

A summary of the method for obtaining the impedance and the wake function is now provided. The equation describing the eigensystem, obtained from the circuit model applied to all N $(= 206)$ cells is given below:

$$\begin{pmatrix} \hat{H} - \lambda U & H_x^t & 0 \\ H_x & H - \lambda U & -G \\ 0 & G & -R \end{pmatrix} \begin{pmatrix} \hat{a} \\ a \\ A \end{pmatrix} = \begin{pmatrix} \lambda B \\ 0 \\ 0 \end{pmatrix}, \tag{1}$$

where $f = \omega/2\pi = 1/\sqrt{\lambda}$ refers to frequency, H $(\hat{H})$ describes TE (TM) modes, H_x^t is the transpose of the cross-coupling matrix (between TE–TM modes), G and R are manifold coupling

matrices and U is an identity matrix. All these individual elements are themselves matrices of dimension $N \times N$. The TE (TM) eigenvectors in the accelerator cavity are given by a ($\hat{a}$) and the TE modes in the manifold by the vector A. The beam excitation is described by the B vector. Furthermore, wall losses are introduced into the analysis by providing a resistor in series with each of the L–C circuits and also in the transmission line that represents the manifold. This adds an imaginary term to the diagonals of the corresponding H-matrices, but it has the benefit of broadening the associated resonant peaks in the spectral function and thus reduces the required sampling of frequency points. To condense notation this is written in the form

$$\left(\bar{H} - \lambda U\right)\bar{a} = \lambda \bar{B}. \tag{2}$$

The three elements of (2) are given by

$$\bar{H} = \begin{pmatrix} \hat{H} & H_x^t & 0 \\ H_x & H & -G \\ 0 & G & -R \end{pmatrix}, \quad \bar{a} = \begin{pmatrix} \hat{a} \\ a \\ A \end{pmatrix} \quad \text{and} \quad \bar{B} = \begin{pmatrix} B \\ 0 \\ -A \end{pmatrix}. \tag{3}$$

The impedance is obtained from

$$Z(\omega) = \frac{1}{2\pi^2} \sum_{n,m}^{N} \sqrt{K_s^n K_s^m \omega_s^n \omega_s^m} \exp[(\mathrm{j}\omega L/c)(n-m)]\tilde{H}_{nm}, \tag{4}$$

where the $3N \times 3N$ matrix $\tilde{H}$ is given by:

$$\tilde{H} = \bar{H}(U - \lambda^{-1}\bar{H})^{-1}, \tag{5}$$

L refers to the length of a single accelerating cell and K_s^n is the single-cell transverse kick factor evaluated at the synchronous frequency $\omega_s^n/2\pi$ for mode n. The transverse wake function (i.e. wake potential per unit length) for a particle trailing a distance s behind a velocity c drive bunch (per unit drive bunch charge per unit drive bunch displacement) may be written as

$$W_\perp(s) = \frac{1}{2\pi} \int [Z(\omega - \mathrm{j}\varepsilon) \exp[(\mathrm{j}s/c)(\omega - \mathrm{j}\varepsilon)]\mathrm{d}\omega. \tag{6}$$

Here ε refers to a small displacement from the real axis and is introduced to broaden the resonant peaks. In the presence of suitable damping, this offset is not required and in practice the introduction of Ohmic damping is sufficient to broaden the resonances sufficiently to enable the impedance to be adequately sampled. Finally, it should be noted that the circuit model introduces a small non-physical precursor signal and in order to minimize this effect a causal wake function is introduced. This consists of subtracting the wake ahead of the bunch, which from causality considerations should be zero [13]. The causal wake function is defined as

$$W_\mathrm{c}(s) = \theta(s)[W_\perp(s) - W_\perp(-s)]. \tag{7}$$

W_c equals $W_\perp$ for $s >$ NL and vanishes for negative s. Here $\theta(\mathrm{s})$ is the unit step function. W_c is a more faithful representation of the wake function in the accelerating structure than the strict equivalent circuit model. From causality for an ultra-relativistic beam there cannot be a wake function ahead of the exciting bunch and therefore $W_\perp(-s)$ for $s > 0$ is identically zero:

$$W_\perp(-s) = \frac{1}{2\pi} \int_{-\infty}^{\infty} Z(\omega + \mathrm{j}\varepsilon) \exp[(\mathrm{j}s/c)(\omega + \mathrm{j}\varepsilon)]\,\mathrm{d}\omega, \tag{8}$$

which leads to

$$W_\perp(s) - W_\perp(-s) = (\pi)^{-1}\mathrm{j}\int_{-\infty}^{\infty} \mathrm{Im}\{Z(\omega - \mathrm{j}\varepsilon)\}\exp(\mathrm{j}\omega s/c)\,\mathrm{d}\omega, \tag{9}$$

$$= \frac{2}{\pi}\int_0^{\infty} \mathrm{Im}\{Z(\omega + \mathrm{j}\varepsilon)\}\sin(\mathrm{j}\omega s/c)\,\mathrm{d}\omega. \tag{10}$$

To include the contribution of poles on the real axis (with real residue) in (9) and (10), we interpret

$$\mathrm{Im}\{(\omega \pm \mathrm{j}\varepsilon - \omega_0)^{-1}\} = \mp\pi\,\delta(\omega - \omega_0) \tag{11}$$

and define $4\mathrm{Im}\{Z(\omega + \mathrm{j}\varepsilon)\}$ as the spectral function $S(\omega)$ of the wake function. Thus, we have

$$W_\mathrm{c}(s) = \frac{\theta(s)}{2\pi}\int_0^{\infty} S(\omega)\sin(\omega s/c)\,\mathrm{d}\omega. \tag{12}$$

We further note that the wake envelope function $\hat{W}(s)$ associated with W_c, representative of the maximum excursion in the wake function, is given by

$$W_\mathrm{c}(s) = \frac{\theta(s)}{2\pi}\left|\int_0^{\infty} S(\omega)\exp(\omega s/c)\,\mathrm{d}\omega\right|. \tag{13}$$

The envelope provides a measure of the worst-case wake function and this proves to be a helpful criterion in designing accelerating structures.

It is interesting to note that the undamped case corresponds to a sum over discrete eigenmodes [13], and is obtained by setting the coupling matrix G to zero, Z is real on the real axis and contains a set of poles on the real axis at the modal frequencies. The spectral function is then a sum of delta functions

$$S(f) = 2\sum_p K_p\delta(f - f_p) = 2K_n\mathrm{d}n/\mathrm{d}f. \tag{14}$$

When the coupling is weak, the position of the resonances can be found by perturbation theory, their distance from the real axis is small compared with their separation, and the spectral function has sharp narrow peaks in place of the delta functions of the undamped case. As the coupling strength increases, these resonances (poles in the impedance) move further from the real axis, the peaks broaden, and while the peaks generally remain quite discernable, the behaviour is relatively smooth. The spectral function can be computed as a function of frequency by direct evaluation of equation (4). A $3N \times 3N$ sparse matrix inversion is involved. In the weak coupling case, it is relatively simple to determine the modal frequencies, eigenvectors and Q values and hence to compute the damped modal sum. In contrast, a large number of frequency points is required to adequately delineate the narrow peaked spectral function. The situation is reversed in the strong coupling case.

We apply this method to calculate the spectral function for RDDS1, including manifold damping and an Ohmic $Q \sim 6500$. The resulting spectral function is shown in figure 6 along with the smoothed, undamped version. The latter corresponds to the idealized case of a Gaussian distribution which although uniformly sampled is truncated at the ends of the structure.

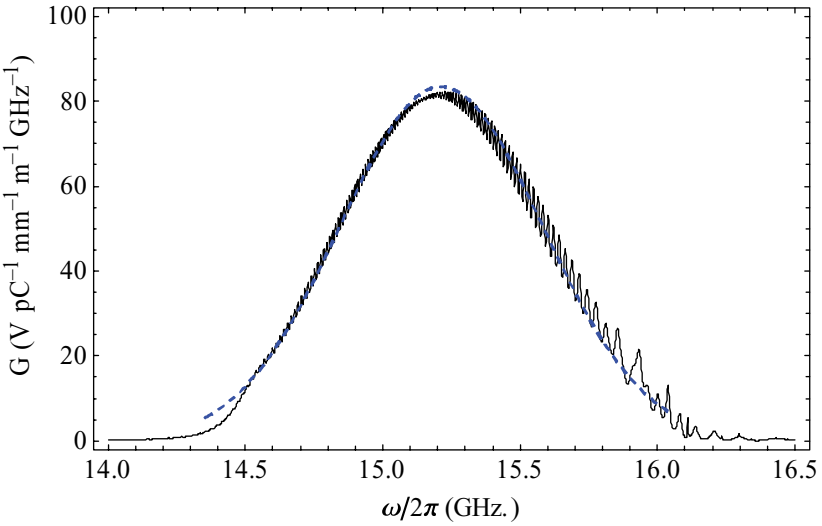

Figure 6. Spectral function indicated by the black solid line for accelerating structure RDDS1 in the absence of fabrication errors. The dashed blue line denotes the smoothed undamped kick factor weighted density function $(2K\,\mathrm{d}n/\mathrm{d}f)$.

In practice N cells are used to produce a finite sampling of the Gaussian design and this together with truncation of the Gaussian will give rise to a wake function with non-Gaussian properties and for this reason the spectral function is required to provide an accurate prediction of the wake function likely to be experienced by an accelerated beam. The corresponding wake function is obtained using equation (13) and displayed in figure 7. Also shown are two additional curves, which denote a structure that excludes the manifold, the detuned structure (DS) structure and a structure that is only provided with copper losses to damp the wake function and no tuning, the Q_{Cu} case. Beam dynamics constraints dictate that the wake function at the first trailing bunch and thereafter, i.e. at 1.4 ns in the NLC design, should be less than 1 V pC^{-1} mm^{-1} m^{-1} and this is achieved for the RDDS1 case.

However, a purely DS gives rise to a recoherence of modes that allows the wake function to rise to about unity. The location of this recoherence is quite predicable as it is given by the reciprocal of the minimum separation of modes in the spectral function, which in this case is ∼8.75 MHz (corresponding to ∼114 ns) and for the DS it is 7 MHz (corresponding to ∼143 ns). Also, the maximum separation of modes, which is located towards the higher frequency ends of the spectral function, predicts the location of the first recoherence. The separation is approximately 111 MHz and this corresponds to 9 ns and, as damping has not acted in this interval, it is the same position for both the DS and damped DS (DDS) structure.

As pointed out earlier, fabrication errors give rise to significant frequency errors and the implications for the wake function are analysed in the next section.

4. Fabrication errors and their influence on wake functions

Fabrication errors result in a shift in the design frequencies of the accelerating structure. In order to predict the wake function resulting from these fabrication errors we mapped all eight

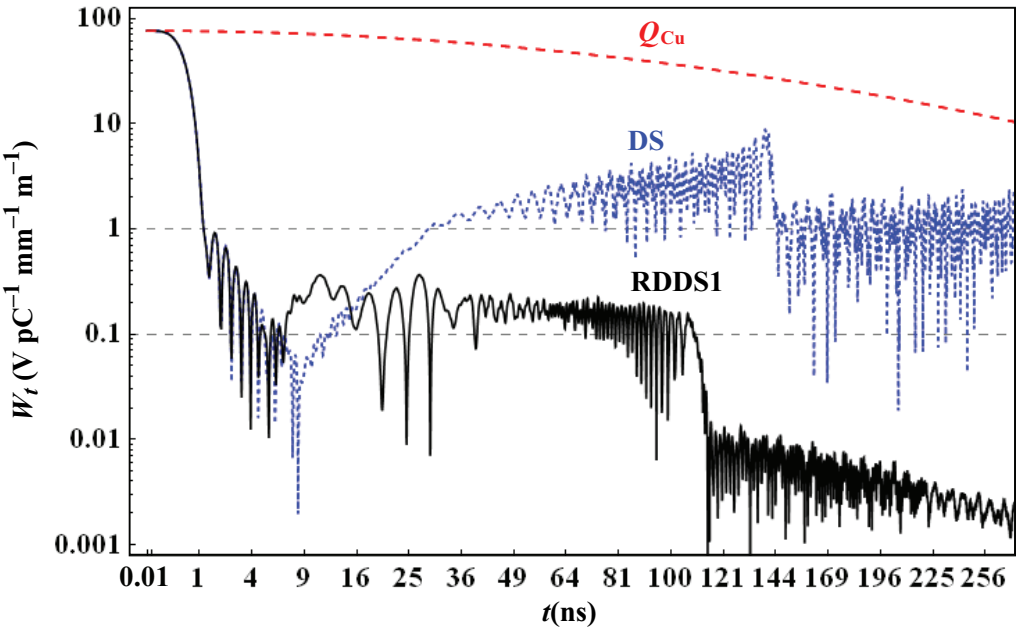

Figure 7. Envelope of the transverse wake function in the absence of fabrication errors. Three methods of wake function suppression are illustrated: damped and detuned wake function (DDS), pure detuning (DS) and pure Ohmic damping (Q_{Cu}).

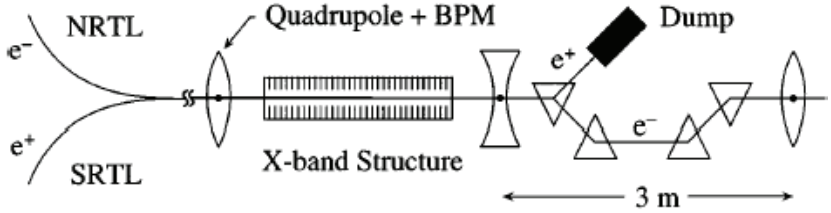

Figure 8. Schematic representation of ASSET facility at the SLAC National Accelerator Laboratory.

parameters for all N cells onto the new frequencies of the cells. This method allows the spectral function and the wake function to be determined rapidly. Even though the errors introduced due to fabrication errors are likely to dilute the damping of the wake function substantially to the extent that it is unlikely that this will be usable as an accelerating structure for linear colliders, we went ahead nonetheless and performed an experiment to determine the wake function. This allows us to determine the accuracy of the circuit model and indeed to assess the influence of experimental fabrication errors.

The wake function was measured using the Accelerator Structure Setup (ASSET) facility in sector 2 of the 2-mile long linac at SLAC and this is shown schematically in figure 8. This essentially consists of a drive positron bunch extracted from the South Damping Ring that excites a wake and a witness electron bunch extracted from the North Damping Ring that is used to monitor the transverse momentum kick. We also conducted parasitic single-beam measurements on the wake function radiated to the manifold ports [19]. However, in this paper,

we restrict ourselves to analysing the wake function excited. During the experiments, the 1.8 m long RDDS1 was maintained at its design operating temperature of 45 °C. The fundamental mode input and output couplers were terminated, either through similar cable connections or a matched load. In the linac, the driving bunch passed through the RDDS1 and was then steered into a dump. The magnet used for this purpose is also the first bend of a chicane that transported electrons back onto the linac axis. The electron bunch served as the witness bunch, and was extracted from the North Damping Ring at a later time and injected on-axis into the linac via the North-Ring-To-Linac (NRTL) transport line. In traversing the RDDS1, the witness bunch was deflected by the wake function generated by the drive bunch. The witness bunch then passed though the chicane and down the linac where its trajectory was recorded by beam position monitors (BPMs) located in each of the quadruple magnets. The transverse wake function was determined by measuring the change in the witness bunch deflection per unit change in the drive bunch offset in the structure. The measurement process was optimized in the vertical plane.

The angular kick imparted to the witness bunch can be obtained by considering the ratio of the transverse to longitudinal energy:

$$\Delta\theta_{\mathrm{y}} = \zeta W_{\perp}(t)\Delta y_{\mathrm{d}}/E_{\mathrm{w}}, \tag{15}$$

where $W_{\perp}(t)$ is the transverse wake function at time t behind the drive bunch, E_{w} ($= 1.2$ GeV) is the witness bunch energy and Δy_{d} is the offset in the drive bunch from the electrical centre of the accelerating structure. The wake function is provided with units of the transverse voltage imparted divided by the product of the total drive charge (en_{d}), drive offset and structure length (L_{s}). These bunches are assumed to be Gaussian and the factor ζ is given by

$$\zeta = e^2 L n_{\mathrm{d}} \exp(-\omega^2\sigma^2/c^2). \tag{16}$$

Here L is the length of the structure, n_{d} is the total number of particles in the drive charge bunch, $\omega/2\pi$ ($= 15.1$ GHz) is the central frequency of the distribution and σ ($= 550\,\mu$m) is the rms bunch length. During operation n_{d} varied from 2×10^{10} to 3×10^{10}.

The resulting experimental measurement of the wake function together with that of the predicted wake for DS and RDDS1 is illustrated in figure 9. The circuit model provides a good prediction of the wake function as the general properties of the wake function are reproduced. The effect of fabrication errors is clearly discernable as comparing figure 9 with figure 7 indicates that the wake function rises above 1 V pC^{-1} mm^{-1} m^{-1} due a shift in the cell frequencies. This is understood by considering the relative size of the frequency shift introduced from fabrication errors compared with the separation of modes and the relative location of the shift. As there is a frequency shift of 35 MHz close to the centre of the structure where the minimum mode separation is 8.75 MHz it is clear that a considerable distortion in the modes will occur.

This enables us to arrive at a design strategy for the suppression of the transverse wake using a damped and DS. To minimize the distortion in the design for wake function suppression, the shift in mode frequencies is required to be a small fraction of the minimum mode spacing for that particular part of the structure. The tolerances are much looser towards the ends of the structure where the mode separation is more than 100 MHz. In practice for linear colliders, the fundamental mode sets require a tolerance of 1 MHz and this leads to a corresponding error in the dipole mode frequencies of approximately 2 MHz that is well below the minimum mode spacing in the centre of the structure, typically a little more than 8 MHz. Thus, provided the overall tolerance on random and systematic frequency errors is kept to within 2 MHz, the wake

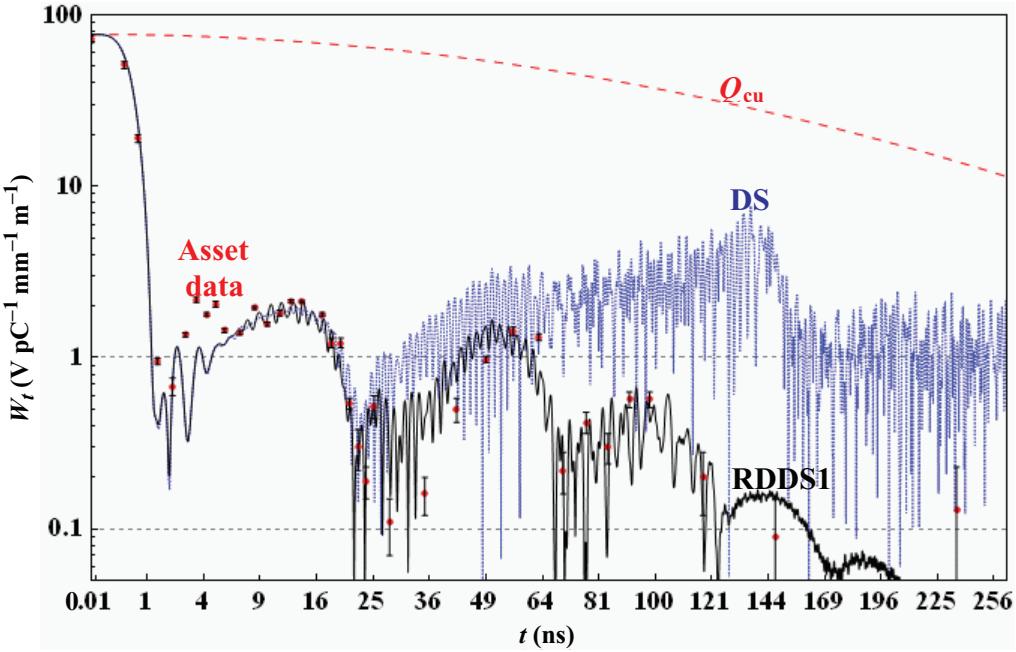

Figure 9. Envelope of the transverse wake function due to frequency errors obtained in fabricating a complete 206-cell structure. The predicted wake function is indicated by the solid black line and the red dots correspond to experimentally determined values. The design goal of 1 V pC^{-1} mm^{-1} m^{-1} and the limit in the accuracy of the measurement of 0.1 V pC^{-1} mm^{-1} m^{-1} are indicated by dashed lines.

function will be properly suppressed with the moderate damping and strong detuning in the RDDS1 design and in similar accelerating structures.

Acknowledgments

The overall program of X-band accelerators for linear colliders has benefited from seamless collaborations with the following main laboratories: SLAC, KEK, Fermi and LBNL. In particular, we would like to single-out the important contributions made by several individuals: K Bane, G Bowden, D L Burke, J Cornuelle, V Dolgashev, Z Farkas, J Frisch, E Garwin, S Harvey, H Hoag, K Jobe, R Kirby, N Kroll, F Le Pimpec, Z Li, G A Loew, J Lewandowski, R J Loewen, D McCormick, R H Miller, C Nantista, J Nelson, C K Ng, R Palmer, E Paterson, C Pearson, N Phinny, M Pivi, T Raubenheimer, M Ross, R D Ruth, T Smith, S Tantawi, P Tenenbaum, K Thompson, P B Wilson, SLAC; H Baba, Y Funahashi, N Higashi, Y Higashi, N Hitomi, H Kawamata, N Kudo, T Kume, H Matsumoto, Y Morozumi, J S Oh, T Shintake, K Takata, T Takatomi, N Toge, K Ueno, Y Watanabe, KEK; T Arkan, C Boffo, H Carter, D Finley, I Gonin, T Khabiboulline, S Mishra, G Romanov, N Solyak, FNAL; J Klingmann, K van Bibber, LLNL; S Doebert, CERN; N Baboi, DESY. This work was supported by the US Department of Energy under contract DE-AC02-76SF00515.

References

[1] *International Linear Collider Technical Review Committee (ILC-TRC) Second Report* 2003 SLAC-R-606
[2] *International Linear Collider Technical Review Final Report* 2004 http://www.linearcollider.org
[3] Brinkman R *et al* (ed) 2001 *The TESLA Technical Design Report* DESY Report 2001–33
[4] Delahaye J P 2000 CLIC – a two beam multi-TeV e+/− linear collider *Proc. XX Int. Linac Conf.* (*Monterey*, *CA*)
[5] Braun H *et al* 2006 Updated CLIC parameters 2005 *CLIC Note 627*
[6] Winick H 1995 *Synchrotron Radiation Sources: A Primer (Series on Synchrotron Radiation Techniques and Applications)* (Singapore: World Scientific)
[7] Padamsee H, Knobloch J and Hays T 2008 *Superconductivity for Accelerators* 2nd edn (New York: Wiley-VCH)
[8] Wiedemann H 2007 *Particle Accelerator Physics* 3rd edn (Berlin: Springer)
[9] Wilson P B 1987 Introduction to wake fields and wake potentials *US Particle Accelerator School, Batavia, IL (SLAC-PUB-4547)*
[10] Yokoya K 1989 Cumulative beam break up in large scale linacs *DESY Report 86-084*
[11] Bohn C L and Delayen J R 1992 Cumulative beam breakup in linear accelerators with periodic beam current *Phys. Rev.* A **45** 5964
[12] Mosnier A 1993 Instabilities in linacs *DAPNIA-SEA-93-19* 55 pp
[13] Jones R M, Adolphsen C E, Wang J W and Li Z 2006 Wake function damping in a pair of X-band accelerators for linear colliders *Phys. Rev. ST Accel. Beams* **9** 102001
[14] Caspers F 1992 *Bench Methods for Beam-coupling Impedance Measurement (Lecture Notes in Physics Frontier in Beams: Intensity Limitations* vol 400*)* (Berlin: Springer)
[15] Bruns W 1997 GdfidL: a finite difference program with reduced memory and CPU usage *Proc. Particle Accelerator Conf. (PAC 1997) Vancouver*
[16] The MAFIA Collaboration 1994 *MAFIA-L 1994* (Darmstadt: CST GmbH)
[17] Li Z *et al* 2004 X-band linear collider R&D in accelerating structures through advanced computing *9th European Particle Accelerator Conf. (EPAC04), Lucerne, Switzerland*
[18] Bane K L F and Gluckstern R L 1993 The transverse wake function of a detuned X-band accelerator structure *Part. Accel.* **42** 123–69
[19] Seidel M, Adophsen C E, Bane K L F, Jones R M, Kroll N M, Miller R H and Whittum D H 1998 Absolute beam position measurement in an accelerator structure *Nucl. Instrum. Methods* A **404** 231–6